

EULER DECONVOLUTION AND SPECTRAL ANALYSIS OF REGIONAL AEROMAGNETIC DATA FROM THE SOUTH-CENTRAL ZIMBABWE CRATON: TECTONIC IMPLICATIONS

¹Ranganai, R. T.

¹Department of Physics, University of Botswana, P.Bag UB0704, Gaborone, Botswana.

Email: ranganai@mopipi.ub.bw

ABSTRACT: Existing regional aeromagnetic data from the south-central Zimbabwe craton has been analysed using 3D Euler deconvolution and spectral analysis to obtain quantitative information on the geological units and structures for depth constraints on the geotectonic interpretation of the region. The Euler solution maps confirm and extend the structural pattern previously identified using shaded relief imaging and derivative techniques: ENE, NNE, NNW, NW and WNW; thus confirming the geological significance of the qualitative interpretation. In places, Euler solutions also show additional patterns typical of sill-edges, thus mapping previously unrecognised mafic/ultramafic intrusions. Most structures identified are predominantly of shallow origin, with Euler depths solutions 1.0 km, and cut across the greenstone belts. A number of isolated deep Euler solutions are associated with ultramafic complexes, the Great Dyke and the Umvimeeela dyke; and these points could represent the original magma chambers and/or feeder points for these units. A linear cluster of solutions with depths around 2.0 km marks the Zimbabwe craton-Limpopo Belt boundary remarkably well. Spectral analysis results suggest the magnetic basement at about 8 km depth, and this probably corresponds to a crustal boundary deduced from gravity and seismic data to occur at 7-9 km depth. The geostructural framework of the area is compatible with the postulated late Archaean collision involving the Zimbabwe and Kaapvaal cratons and the Limpopo Belt, and later crustal extension during the break-up of Gondwana. The geological-tectonic correlation suggests that the interpreted regional trends are mainly 2.6 Ga and younger; and relate to tectonic events including the reactivation of the Limpopo Belt at 2.0 Ga and the major regional igneous/dyking events at 1.8-2.0 Ga (Mashonaland), 1.1 Ga (Umkondo) and 180 Ma (Karoo). The greenstone belts were an integral part of the lithosphere before much of the upper crustal (brittle) deformation occurred.

Key words: Aeromagnetic data, Euler deconvolution, Spectral analysis, Tectonic interpretation, Zimbabwe craton

INTRODUCTION

The south-central region of the Archaean Zimbabwe craton (ZC) encompasses several geological features: basement gneisses and tonalites of the ~3.5 Ga Tokwe Segment, greenstone belts, the Great Dyke and its satellites, the North Marginal Zone (NMZ) of the Limpopo belt, post-volcanic granite plutons, and mafic dyke swarms as shown in Fig. 1 [Wilson, 1981; 1990; Wilson et al., 1987; 1995; Bickle and Nisbet, 1993]. The ~3.5 Ga Tokwe Segment (TS, index map in Fig. 1) is a unique terrain considered to be a nucleus, from where the craton grew westwards and

northwards by crustal accretion (Wilson, 1990; Wilson et al., 1995; Kusky, 1998; Horstwood et al., 1999; Jelsma and Dirks, 2002). The study area is therefore considered of crucial importance to the understanding of the tectonic evolution of the craton as a whole, the Limpopo belt, and the Archaean crust in general (e.g., Nisbet, 1987; Wilson, 1990; Bickle and Nisbet, 1993; Fedo et al., 1995; Kusky, 1998; Horstwood et al., 1999; Jelsma and Dirks, 2002). Consequently, many geological studies have been carried out in this regard and these have been complemented by geophysical investigations at various stages (e.g., Podmore and Wilson, 1987; Gwavava, et al., 1992; Jones et al., 1995;

Euler Deconvolution and Spectral Analysis of Regional Aeromagnetic Data from the South-Central Zimbabwe Craton: Tectonic Implications

Mushayandebvu, 1995; Ranganai, 1995; Ranganai et al., 1995, 2008). The geophysical studies involve gravity and aeromagnetic data, and a number of greenstone belt gravity models have been derived (Ranganai et al., 2008). However, the aeromagnetic studies have so far only provided a qualitative interpretation with an indication of where changes in magnetic susceptibility occur, but not what

produces the anomaly nor its depth (e.g., Ranganai et al., 1995; Ranganai and Ebinger, 2008). Typically, the most common parameter sought for in aeromagnetic interpretation is the location of the magnetic source bodies and their depths (Bournas et al., 2003 and references therein).

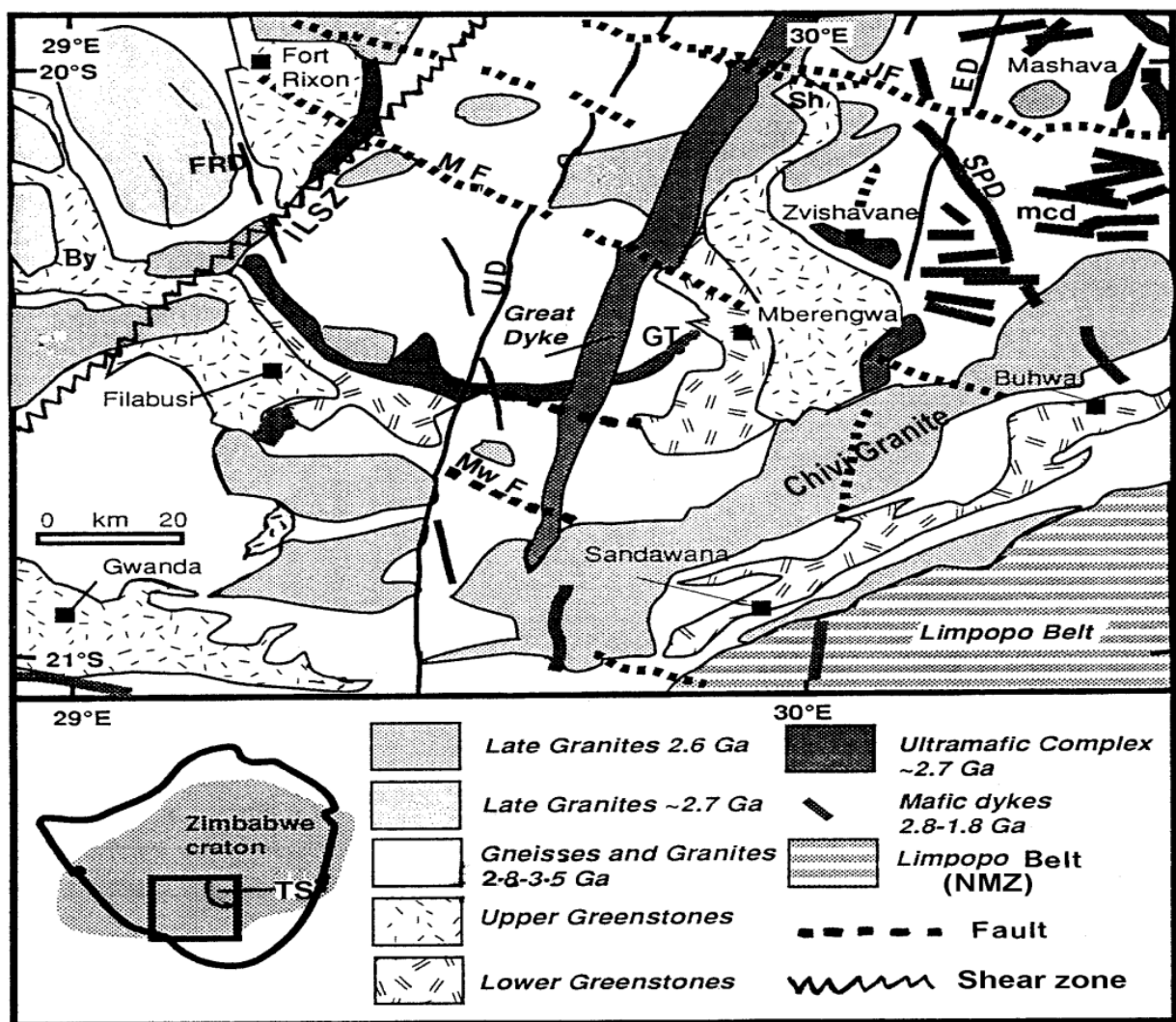


Figure 1. Simplified geological map of the study area. Greenstone belts are named after respective towns (By = Bulawayo). Other units are: TS (see insert) = ~3.5 Ga Tokwe Segment (north-eastern area between Zvishavane and Mashava), ED = East dyke, GT = Gurumba Tumba serpentinite; mcd = Mashava-Chivi dykes, SPD = Sebang-Poort dyke, UD = Umvimeela dyke, ILSZ = Irisvale-Lancaster Shear Zone, JF = Jenya fault, MF = Mchingwe fault, Sh = Snake-head section (Mberengwa belt), MwF = Mwenezi fault, FRD = Fort Rixon dykes.

In this paper, existing regional aeromagnetic data are used to estimate the location and depths to susceptibility discontinuities through standard 3D Euler deconvolution and spectral analysis techniques (e.g., Spector and Grant, 1970, 1975; Hahn et al., 1976; Thompson, 1982; Ruotoistenmaki, 1983, 1987; Reid et al., 1990). The paper extends the preliminary investigations of Ranganai (1999). The main objectives are to provide depth constraints on previous qualitative structural interpretation using shaded relief imaging and derivative techniques. These data-enhancement techniques present maps in a form which assists human comprehension through recognition of special patterns while the present study provides quantitative information for geological interpretation. The application of Euler's homogeneity relation through the process of deconvolution has been demonstrated to be an effective method for delineation of potential field boundaries and the estimation of depth to their upper edges (e.g., Reid et al., 1990; McDonald et al., 1992; Paterson et al., 1992; Mushayandebvu et al., 2001, 2004; Bournas et al., 2003). Spectral analysis has been commonly applied for the determination of depths of magnetic assemblages within the upper crust, depth to magnetic basement and/or crustal thickness variations (e.g., Hinze, 1985; Cowan and Cowan, 1993; Poudjom-Djomani et al., 1995; Allek and Hamoudi, 2008). Both techniques are therefore useful for investigating structures, magnetic zones, and crustal domains previously identified in the area (Ranganai, 1995; Ranganai et al., 1995, 2008). The computed depths constitute important quantitative constraints on the geological interpretation of the area, and the elucidation of its tectonic evolution; they help discriminate geotectonic models.

GEOLOGICAL SETTING

The study area is the south-central part of the Archaean Zimbabwe craton and lies between latitudes 19.9°S and 21.1°S and longitudes 28.9°E and 30.5°E, with mining towns located throughout the area (Fig. 1). Principal geological units in the study area include the Mberengwa (Belingwe), Buhwa, Filabusi, Fort Rixon and Gwanda greenstone belts, 'young' K-rich (post-volcanic) granites, and sections of the Great Dyke and its satellites (Umvimeela and East dykes), set within ancient tonalitic gneisses (Fig. 1). The 'young' granite plutons (2.7-2.6) intrude and deform both the older gneisses and the greenstone belts (Wilson et al., 1995; Jelsma et al., 1996; Horstwood et al., 1999), but these are in turn cut by the ~2.5 Ga NNE-striking Great Dyke and its nearly parallel satellite dykes and features. The Great Dyke is a linear mass of mafic-ultramafic rocks while its satellites are true gabbroic dykes (Wilson and Prendergast, 1988; Oberthür et al., 2002); together they form the first

major igneous event after cratonization (e.g., Wilson, 1990; Hortswood et al., 1999; Jelsma and Dirks, 2002; Schoenberg et al., 2003). Many workers argue for a close relationship between the emplacement of the Great Dyke and satellites, the intrusion of the late plutons and tectonic events in the Limpopo belt (e.g., Mukasa et al., 1998; Frei et al., 1999; Oberthür et al., 2002). Several layered ultramafic intrusions of the ~2.8 Ga Mashava Ultramafic Suite (Wilson, 1979, 1981, 1990; Prendergast and Wingate, 2007) and mafic dykes of various ages are scattered throughout the area (Wilson et al., 1987). They both appear to be intimately related to the tectonic processes that produced the main Archaean granite-greenstone terrain (Wilson, 1981, 1990; Wilson et al., 1995).

Greenstone stratigraphy includes the ~2.9 Ga Lower Greenstones, the dominant/widespread 2.7 Ga Upper Greenstones and minor ~2.7 Ga Shamvaian type sediments (Wilson, 1981, 1990; Taylor et al., 1991; Bickle and Nisbet, 1993; Wilson et al., 1995; Jelsma et al., 1996; Horstwood et al., 1999). Generally, all the greenstone belts show a characteristic sequence of ultramafic, mafic, felsic and volcanic-sedimentary assemblages, mainly at greenschist facies metamorphism rising to amphibolite facies at their margins, close to batholith contacts. The Mberengwa (Belingwe) greenstone belt (Fig. 1) contains the most complete greenstone sequences in the craton, and its well preserved and exposed stratigraphy has been correlated with units across much of the craton (Wilson, 1979, 1981; Bickle and Nisbet, 1993; Wilson et al., 1995; Jelsma and Dirks, 2002; Prendergast, 2004). The greenstone sequences and configuration may reflect rifted or overplated sequences related to emplacement of mantle plumes, with deformation being attributed to vertical tectonic processes, or remnant oceanic crust or island-arc material that was amalgamated with continental fragments during some form of subduction-accretion (Jelsma and Dirks, 2002; Ranganai et al., 2008). Detailed revisions of the greenstone stratigraphy can be found in Wilson et al. (1995) and Hortswood et al. (1999) while comprehensive summaries of the craton are given by Blenkinsop et al. (1997) and Jelsma and Dirks (2002). Campbell et al. (1992) provide a provisional tectonic map and tectonic evolution of the country.

The study area is bounded on its south-eastern edge by the Northern Marginal Zone (NMZ) of the Archaean Limpopo orogenic belt (LB), in thrust contact with cratonic granitoids (Rollinson and Blenkinsop, 1995; Mkweli et al., 1995; Fedo et al., 1995; Frei et al., 1999). The NMZ may consist mainly of reworked granitoid-greenstone rocks of the craton at amphibolite facies metamorphism (Hickman, 1978; Van Reenen et al., 1992), with several inclusions of

Euler Deconvolution and Spectral Analysis of Regional Aeromagnetic Data from the South-Central Zimbabwe Craton: Tectonic Implications

mafic dykes, ultramafics and banded iron formation (Rollinson and Blenkinsop, 1995). The ZC-NMZ boundary is traditionally taken as the orthopyroxene isograd but recent geological mapping points to a tectonic break (Mkweli et al., 1995; Rollinson and Blenkinsop, 1995; Blenkinsop et al., 1995). It is hoped that this study will contribute in-depth information that will help elucidate the nature of the contact previously defined by aeromagnetic signatures alone (Ranganai, 1995; Ranganai et al., 1995).

AEROMAGNETIC DATA AND CORRELATION OF ANOMALIES WITH GEOLOGY

The aeromagnetic data used in this study were obtained from the Zimbabwe Geological Survey (ZGS) and are based on 1 km spaced flight lines with 305 m constant mean terrain clearance. Two surveys were conducted in 1983 and 1988 using Geometrics proton precession (0.1 nT resolution) and Scintrex cesium vapour (0.001 nT resolution) magnetometers, respectively. Flight directions were E-W and/or N-S, approximately perpendicular to the dominant

geological trends, the greenstone belts. Tie-lines were flown 14 km apart and the data were diurnally corrected and flight line-levelled using a combined computer-manual method. Data from the two surveys were combined following the procedure discussed by Barritt (1993). The levelled flight line data were first gridded in the UTM co-ordinate system at 250 m cell size using a bidirectional algorithm (e.g., Smith and Wessel, 1990), and then reduced to the pole. Reduction to the pole (RTP) assumes induced magnetisation and shifts the anomalies to lie directly over the sources (e.g., Blakely, 1995), thus producing anomaly maps that can be more readily correlated to the surface geology. RTP is also a requirement for the Euler deconvolution and spectral analysis algorithms used in this study (Spector and Grant, 1970; Geosoft, 2004; see Appendix). The Geosoft algorithms used to calculate the RTP cater for both high and low magnetic latitudes (-60 in the study area). The RTP data were then contoured at 50 nT interval (Fig. 2) and sunshaded (Fig. 3) for geological and structural mapping before the deconvolution and spectral analysis.

In general, the pole-reduced aeromagnetic data display a

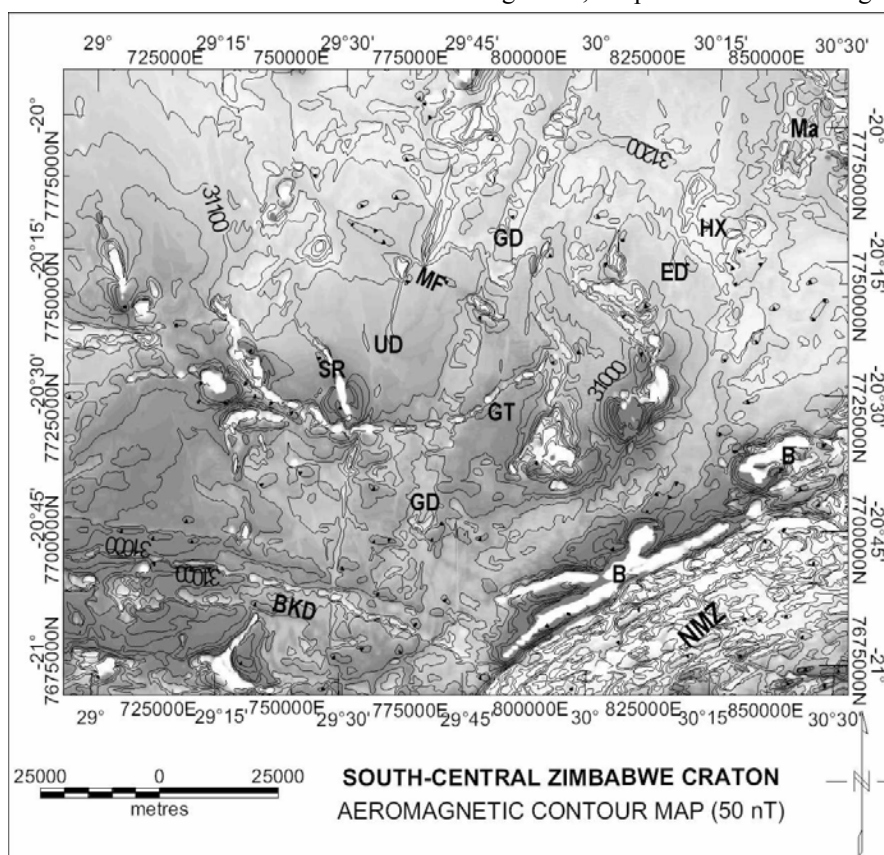


Figure 2. RTP aeromagnetic contour map with grey-scale grid. Basic contour interval is 50 nT. Dark tones represent low values while white tones are high values. Prominent magnetic units are labelled: GD= Great Dyke, B=Buhwa greenstone belt (BIF quartzite); BKD= Botswana Karoo Dyke (swarm); Ma= Mashava (ultramafic) Suite; HX= Interpreted ultramafic body; SR= Shamba (ultramafic) Range; NMZ = North Marginal Zone (Limpopo belt); other labels as in Figure 1

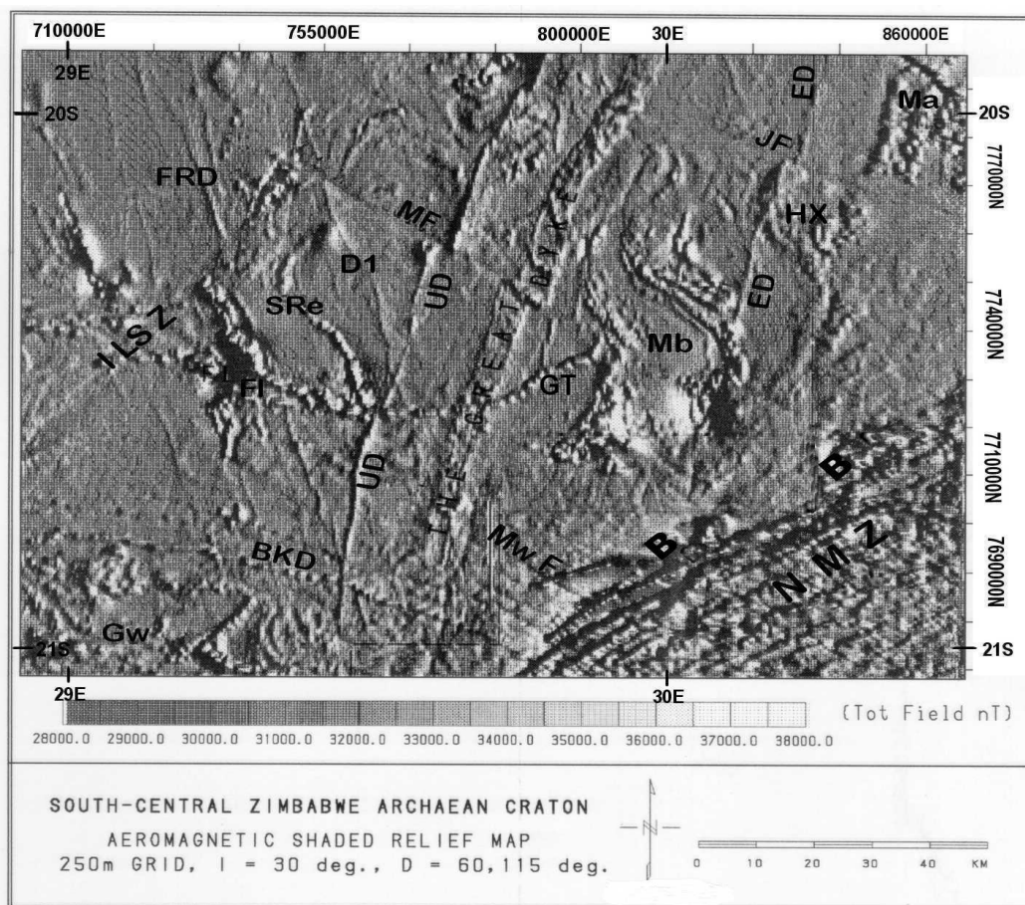


Figure 3. Shaded relief RTP magnetic map of study area. 'Sun' illumination angle is 30 and declination angles are 60, 115. Note the use of two declination angles in order to display the magnetic data which reflect structures at many orientations. Structural features labelled are discussed in text: D1 = dyke; ILSZ = (Irisvale-Lancaster) Shear Zone; SRe = Shamba (ultramafic) range extension; Gw = Gwanda greenstone belt; Mb = Mberengwa (Belingwe) greenstone belt; other labels as in Figs. 1 and 2). Note the dominance of NNW (FRD dyke) and NNE (Great Dyke) dyke trends and NW to WNW fault directions

typical granite-greenstone signature, and anomalies correlate well with geological units: the shapes are clearly outlined and broad lithological boundaries are discernable (cf. Figs. 1 and 2, 3). In all greenstone belts, the extensive Upper Greenstone basalts are characterised by flat, homogeneous relief as the volcanic lavas contain little magnetite and also probably due to the low metamorphic grade. The only exception is the Buhwa greenstone belt (B, Fig. 2) with high magnetic anomalies due to the magnetite, quartzite and haematite which dominate the lithologies (Fedo et al., 1995). Magnetic highs occur over mafic dykes and ultramafic intrusions (e.g., GD, Ma, SR) as well as komatites and banded iron formation horizons within greenstone belts (white tones in Figure 2). Three or four different magnetic zones can be identified on the RTP contour map (Fig. 2) based on anomaly textures, defined by parameters like linearity, relief, and background level, and features such as anomaly shapes and wavelengths.

The northern half of the study area is generally characterised by relatively high magnetic signatures (~31300 nT) and appears to be a separate terrain. The central and south-central parts have intermediate anomalies (~31000 nT) while the southwest and southeast areas have low (30000 nT) and bipolar (very high, ~32500 nT and low, ~30000 nT) signatures, respectively (Fig. 2).

The latter occur over the Buhwa greenstone belt and the NMZ, reflecting the high metamorphic grade of the area (e.g., Grant, 1985), and possibly the effect of mafic-ultramafic-BIF inclusions in the gneisses. The northern edge of this broad high marks the ZC-LB boundary remarkably well. The four different magnetic zones probably represent crustal domains or magneto-tectonic provinces, and a more detailed qualitative interpretation and discussion is underway.

Euler Deconvolution and Spectral Analysis of Regional Aeromagnetic Data from the South-Central Zimbabwe Craton: Tectonic Implications

Overall, the aeromagnetic data display a considerable range of wavelengths and amplitude variations but are dominated by high amplitude, short wavelength anomalies from shallow sources (Fig. 2). The latter are clearer on shadow and derivative maps (e.g., Fig. 3; Ranganai and Ebinger, 2008) and are expected to be clearly isolated by the gradient based 3D Euler deconvolution technique (e.g., Mushayandebvu et al., 2001; see below and Appendix). Several new features and/or extensions of known units are observed, such as NNW-striking dykes (FRD, D1), ESE-trending dykes (BKD), Shamba Range (ultramafic) extension (SRe), and a possible ultramafic body (anomaly HX) (cf. Figs. 1 and 3). The latter magnetic body (HX) has an associated Bouguer gravity high (Ranganai et al., 2008), thus pointing to a probable ultramafic composition/origin for the anomaly source. Euler deconvolution is applied particularly to quantitatively identify the boundaries of such magnetic entities, and other features.

3D Euler Deconvolution and Structural Mapping

In order to investigate the source of the magnetic lineaments seen on shadow and derivative maps (e.g., Fig. 3), and to confirm the position, structure and/or geological association in previous qualitative interpretation (e.g., Ranganai et al., 2008), Euler deconvolution was applied to provide additional 3D information. The technique is less subjective than shaded relief maps commonly used in locating low gradient anomalies, and it also assists in the delineation of crustal blocks with different magnetic parameters and, therefore, tectonic interpretation (e.g., Bournas et al., 2003). It is particularly useful where there are interfering sources such as in the study area, as it involves the analysis of gradients. However, it should be noted that the depth estimates provided by this method are inherently less well determined than the positional estimates (e.g., McDonald et al., 1992; Mushayandebvu et al., 2001). Further, although it has been claimed that no geological model is assumed (Thompson, 1982; Reid et al., 1990), the optimal use of the algorithm depends to a large part on the user's *a priori* knowledge of the geology in an area. Its successful application also depends on the quality of the data, as well as the selection of the processing parameters, namely: the structural index, N and the grid window size, W (see Appendix). N is a measure of the fall-off rate of the anomaly with distance, and is closely related to the geometry of the causative body with simple bodies having prescribed values, between 0 and 3, as discussed by Reid et al. (1990). We note that the conventional technique used in this study (Reid et al., 1990) assumes that the observed field in each Euler window is due to a 3D source and this leads to generally poorly constrained solutions where the source is in fact 2D (Mushayandebvu

et al., 2004). The various improved versions (e.g., Fairhead et al., 1994; Barbosa et al., 1999; Mushayandebvu et al., 2001, 2004) were not available for this study and therefore the results are not fully 'cleaned out'.

Based on spatial observations from the RTP and derivative maps, a number of structural indices (SI's) and window sizes were applied. In general the number of solutions from the RTP magnetic grid increased as the structural index was increased from SI = 0 to SI = 3, and window size was also increased from 4 (1x1 km) to 12 (3x3 km). When the SI used was between 0 (contact of considerable depth extent) and 1 (dyke or sill edge), the solutions obtained tended to be of shallow depth. At higher values of SI (SI = 1 to 2), the solutions exhibited a clear focus in the location and depth of the solutions, and results for these indices tend to be similar (e.g., Figs 4 and 5). This emphasises the need to apply several structural indices, particularly in geologically complex areas such as are under study. This was also noted by Reid et al. (1990) who suggested that gross structural trends could still be outlined even with a poor choice of N (albeit with inaccurate depth solutions). It should also be noted that due to the gridding process which often results in 'strings of pearls' for dykes (e.g., BKD, Figs. 2 to 5), the dyke anomalies could resemble a line of dipoles, which has a structural index of 2 (Reid et al., 1990; Paterson et al., 1992; Mushayandebvu et al., 2004).

The results of standard Euler deconvolution are as shown in Figures 4 and 5. For a given N and W , the technique calculates from the magnetic gradients in the x , y , and z direction the boundary of a magnetic unit and the depth to the boundary. The located boundary point is plotted on a map and represented by a circle, whose size is scaled according to the depth units. The Euler solution maps presented (Figs. 4 and 5) indicate several structures, with a direct coincidence of linear clustering solutions with known features such as the Umvimeela dyke (UD), the Great Dyke (GD), and the Grumba Tumba serpentinite (GT), and these form obvious features on all maps (cf. Fig. 1). The latter is an outstanding semi-circular (arc-shaped) feature at the centre of the maps, that partly follows the Mwenezi fault (Mw) in the west, cutting across the Great Dyke to terminate against the Mchingwe fault (MF) to the east (Figs. 4 and 5). The widths of these known features are also represented well, particularly at small SI where, for example, both edges of dykes are clear (cf. Figs. 1 and 4). Some linear solutions are traceable for tens of kilometres to just over 100 kilometres (e.g. ED, UD, FRD, BKD; Figs 4 and 5), but others are broken up into segments. Faults can be interpreted at these breaks, but the longer breaks may represent zones of constant susceptibility. Other anomalies are much shorter but the various segments form part of



Figure 4. Euler solution map for RTP magnetic grid; $N=1$, $W=8$ (2×2 km). Acceptance level set at 70%. Features and/or trends discussed in text are labelled

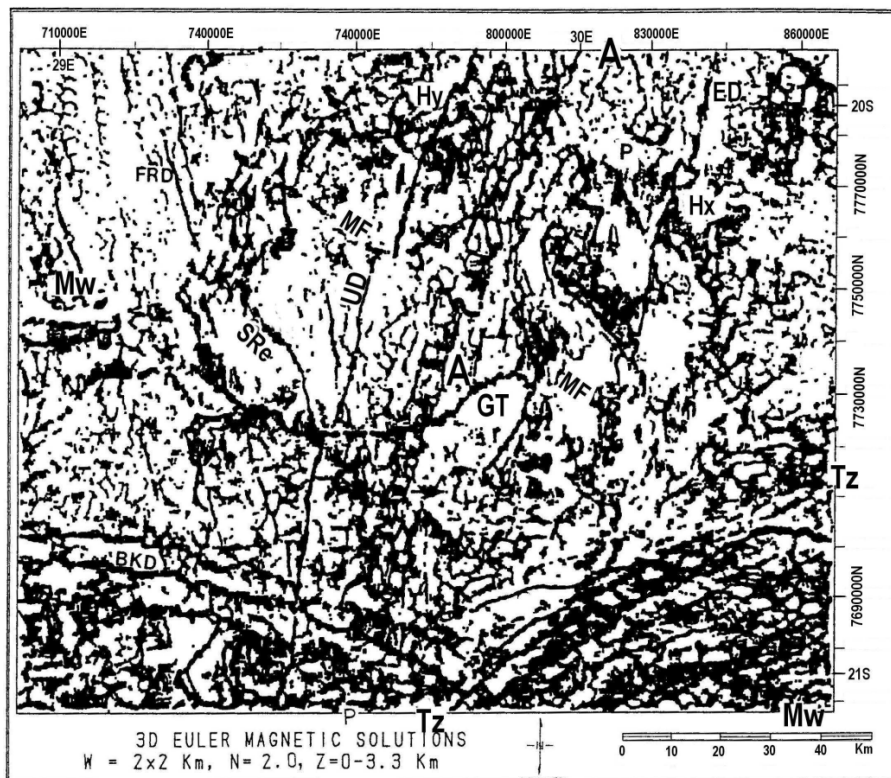


Figure 5. Euler solution map for RTP magnetic grid; $N=2$, $W=8$ (2×2 km). Acceptance level set at 60%. Features and/or trends discussed in text are labelled. Note the general similarity of solution patterns with Figure 4 ($N=1$)

Euler Deconvolution and Spectral Analysis of Regional Aeromagnetic Data from the South-Central Zimbabwe Craton: Tectonic Implications

more continuous features (e.g., MF, Mw; Figs. 4 and 5). These are best viewed at certain directions with the map in hand, allowing their identification as continuous trends and/or significant structures of considerable strike. Others can only be interpreted in conjunction with the magnetic derivative and shaded relief maps (e.g., Fig. 3).

Several other observations can be made from the maps. For example, a number of solutions in the northern area exhibit patterns typical of sill-edges (e.g., HX and HY on Figs. 4 and 5). The Euler deconvolution indicates that the body situated at HY extends to 2.0 km and coincides with a palaeomagnetic interpreted magma source for the Umvimeela dyke (Bates and Mushayandebvu, 1995). Newly found NNE- to NE-trending structures are indicated, particularly in the Mberengwa greenstone belt area (e.g. trends marked AA and PP on Figs. 4 and 5). The Mwenezi fault (Mw F, Figs. 1 and 3) can be extended in both directions from the mapped exposure to cut across the entire study area and into the Limpopo Belt in the south-east (Mw-Mw, Figs. 4 and 5). The ZC-NMZ boundary is

characterised by a distinct linear clustering of solutions on all maps (feature Tz, Figs. 4 and 5). This confirms recent geological interpretations that the boundary is a tectonic break/contact (e.g. Mkweli et al., 1995; Blenkinsop et al., 1995; Rollinson and Blenkinsop, 1995; Ranganai, 1999), rather than the orthopyroxene isograd previously used. Unfortunately, the present results cannot distinguish between a vertical and a thrust contact, but recent advances in the technique may allow the estimation of dip of the magnetic body (e.g., Mushayandebvu et al., 2001, 2004). Several other linear solutions, corresponding to mafic, ultramafic and iron formation inclusions can also be identified within the NMZ. Surprisingly, magnetic zones (briefly discussed above) previously identified on the RTP and apparent susceptibility maps (Ranganai, 1995; Ranganai and Ebinger, 2008) are not represented in any recognisable pattern on the solution maps. This partly confirms the interpretation that the zones reflect relatively deep crustal blocks, although the effect of window size cannot be ruled out.

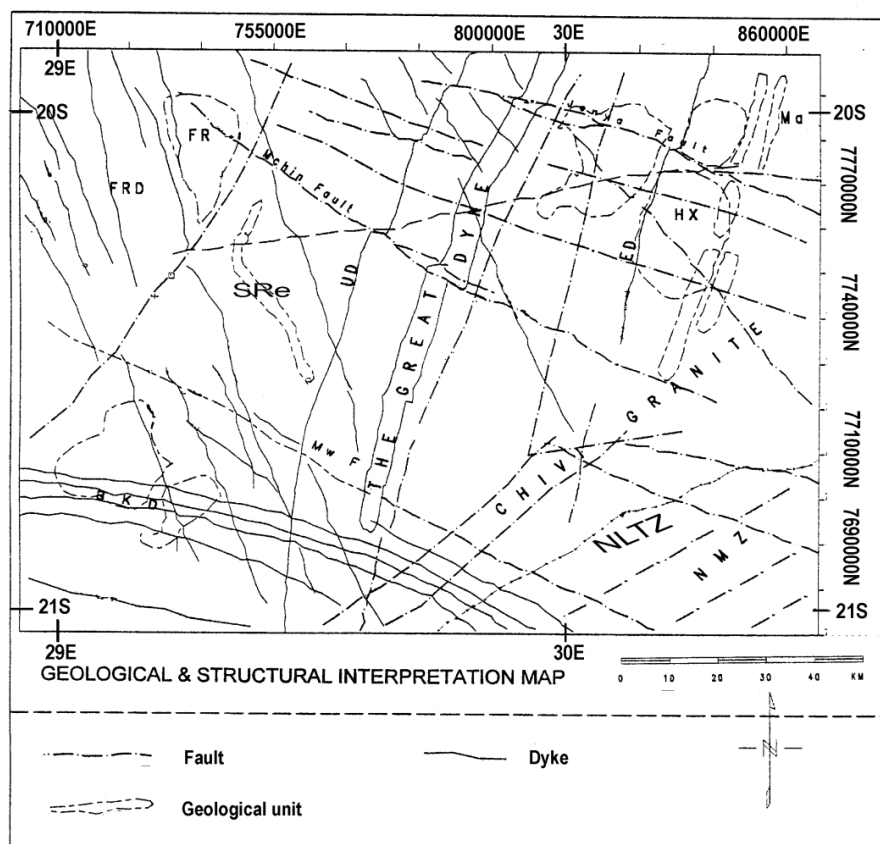


Figure 6. Geological and Structural Interpretation map of the study area (see Figure 1 and Table 1 for comparison). BKD = Botswana Karoo dykes; ED = East dyke, FRD = Fort Rixon dykes, HX = Interpreted ultramafic complex; SRe = Shamba Range extension; UD = Umvimeela dyke, Mchin Fault = Mchingwe fault, Mw F = Mwenezi fault, NLTZ = North Limpopo Thrust Zone. Other geological unit labels (FR, Ma and NMZ) for reference purposes only (cf. Fig. 3)

The final interpretation (Fig. 6) was guided by printed colour maps at various scales and 'on screen' displays with higher resolution than figures presented. It is a compilation of (a) known structures, (b) anomalies calibrated by surface geology, and (c) structures interpreted by analogy to (b). Generally, the western half of the study area is characterised by NNW-trending structures, in places cut by NW-to-WNW-trending faults whereas the east is dominated by NNE-trending structures, in places cut by NW-to-WNW-trending faults and NNW-trending dykes (e.g. Figs. 2 to 6). The southern part shows EW-to-ESE-trending dykes in the west and ENE-trending structures in the east. Significantly, the observed magnetic trends have representatives craton-wide, which implies that our interpretation and inference can be applied to the rest of the craton with some degree of confidence. Relative ages of the structures can be inferred from the details of the intersection relationships and other geochronological information (e.g., Taylor et al. 1991; Wilson et al., 1995; Horstwood et al., 1999; Jelsma and Dirks, 2002; Oberthür et al., 2002; see discussion below).

Euler Depth Solutions and their Significance

In general, the minimum depths returned in Euler deconvolution are of the order of the grid interval, while the maximum depths are about twice the window size (Reid et al., 1990; Geosoft, 2004). In this study, however, comparable solution depths were obtained from different window sizes and structural indices, probably implying the 'true' depths of features. At low values of N ($SI = 0$ to 1), the solutions tended to be shallower than for higher values of N ($SI = 1$ to 2), confirming the out- and sub-cropping nature of several linear features represented by the low SI s. To allow depth investigations for some individual units, solutions have been plotted as circles scaled for the depth magnitudes and subdivided into three levels represented by different sizes (Fig. 7). More than seventy five percent of the depth solutions are less than or equal to 1.0 km, and very few are over 2 km. This means that most of the features mapped are shallow, more so if we have to consider the fact that solution depths using a low SI cluster near the mid-point of a steep feature (McDonald et al., 1992). These shallow structures (particularly ≤ 150 m) are considered important for regional groundwater exploration, and therefore the technique could be used to assess such structures and features in the region (e.g., Ranganai and Ebinger, 2008). The intermediate (1-2 km)

and deeper solutions occur mainly in the southern part of the area: at the ZC-NMZ boundary in the south-east, and over the Gwanda (Gw) greenstone belt area in the south-west (cf. Figs. 1 and 7). A few also occur over ultramafic and mafic intrusions, where there are well-defined anomalies (e.g., Ph, S, D, HX in Fig. 7). The two isolated deepest solutions are associated with ultramafic complexes (Ph and S, Fig. 7), and these points could represent the original magma chambers.

Using the various Euler solution maps, the magnetic sources in the northern parts of the area generally appear shallower than in the southern parts. This suggests that either the sources were emplaced at shallow levels or that the north probably experienced more uplift and higher erosion levels than the south. The latter is supported by the fact that the northern part of the Mberengwa (Belingwe) greenstone belt (Sh, Fig. 1) is considered to be a deeper level crustal section than the main belt to the south (Martin, 1978; Bickle and Nisbet, 1993). This is reported to be at higher grade metamorphism (amphibolite facies) than the main belt (greenschist facies). Based on geological and geophysical evidence, Ranganai et al. (1995) infer that the area underwent at least one major period of heating and uplift, followed by erosion. Magnetic modelling of profiles in several places across the Umvimeela and East dykes within the study area show a progressive increase in depth to top from north to the south (Mushayandebvu, 1995). Both dykes have shallow dips south of latitude $20.5^\circ S$. This, together with palaeomagnetic data, was interpreted to suggest a tilting of the craton adjacent to the Limpopo belt, with the affected block being limited by the cross-cutting Mchingwe fault (Mushayandebvu, 1995).

However, the Great Dyke and its satellites are seen to have isolated areas having slightly deeper solutions of 1.5 to 2.0 km within the northern parts of the area. For the Great Dyke, the area of deep solutions (A, Fig. 7) approximately coincides with the boundary of the Wedza and Selukwe complexes (Wilson and Prendergast, 1988), but it is not yet possible to place any significance to this. A similar area (D) occurs on the Umvimeela dyke (Fig. 7). On this dyke (UD), another area of deep solutions just north of the Mchingwe fault (F, Fig. 7) correlates with a point interpreted as its possible feeder point, identified through magnetic fabric analysis (Bates and Mushayandebvu, 1995). Note that D also encompasses solution patterns typical of sill edges like HX, and could therefore be a concealed ultramafic body.

Euler Deconvolution and Spectral Analysis of Regional Aeromagnetic Data from the South-Central Zimbabwe Craton: Tectonic Implications

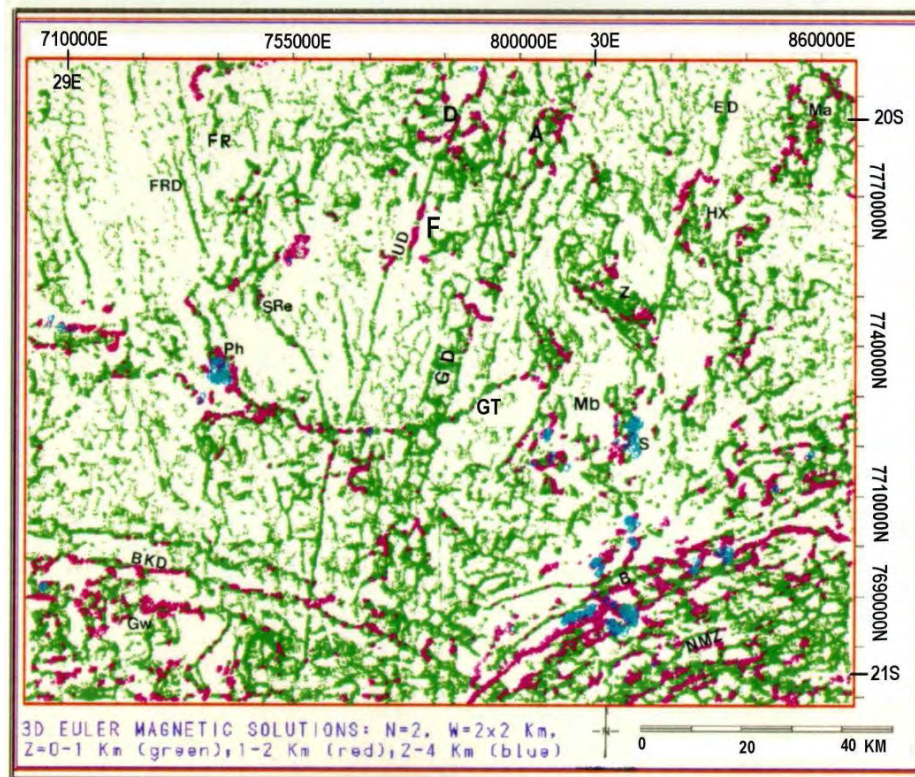


Figure 7. Euler depth solution map for RTP magnetic grid; N=2, W=8 (2 x 2 km). Solution depths: green = 0-1 km, red = 1-2 km, and blue = 2.0-4.0 km. Acceptance level set at 60%. Features and/or trends discussed in text are labelled. (For interpretation of the references to colour in this figure legend, the reader is referred to the web version of this article)

Source Depth Estimates from Magnetic Spectra

Since the aeromagnetic anomaly patterns are shaped very largely by the depths and volumes of the sources (Spector and Grant, 1970), and of course, their magnetisation, mean depths to the sources can be determined by spectral analysis (Ruotoistenmaki, 1983, 1987). The algorithm used for RTP produces a 2D radially averaged power spectrum as a function of wavenumber (cycles/km). [The amplitude spectrum is a 2D function of the amplitude relative to wavenumber and direction, while the radially averaged power spectrum is a function of wavenumber alone.] We use the method of Spector and Grant (1970) where the earth is modelled as an ensemble of rectangular, vertical-sided parallelepipeds of varying depth, width, thickness, and magnetisation. For such a model, the average ensemble depth h is simply half the gradient on the log radial spectra (Appendix). For wavenumbers in cycles/km h is then calculated from the relation (Spector and Grant, 1970):

$$\text{slope} = -4\pi h \tag{1}$$

Best-fit straight lines are drawn on the spectra. In general, there are limitations and errors on the depth estimates due to the window size, the grid spacing and the quality of the linear fit on the plots (e.g., Spector and Grant, 1970; Ruotoisenmaki, 1983, 1987; Poudjom Djomani et al., 1995; Allek and Hamoudi, 2008). For example, the data length must be six times the maximum source depth, and the shallowest depth estimate must be not less than 40% of the grid spacing (see Poudjom Djomani et al., 1995 and references therein).

Figure 8 shows the 2D radially averaged power spectrum of the RTP aeromagnetic data of the study area. The plot shows a small degree of curvature, rather than purely straight line segments. There are several possible reasons for this curvature. It could be due to leakage back into the Nyquist interval, but this is difficult to ascertain, and we suggest that this indicates increasing values of mean depth of ensembles. Ruotoisenmaki (1983, 1987) attributes such problems to the size effect (Appendix) in the method that is used here (Spector and Grant, 1970), particularly if there are areas with consistently varying depths. This leads to

interpreted depths that are larger than the source depths (Spector and Parker, 1979) and, therefore, the computed depths should be considered as maximum depths. It should also be noted that the depths estimated from the aeromagnetic spectra are relative to the flight altitude (305 m in this case).

It is possible to distinguish the residual and regional components in Fig. 8, although the former shows a range of possible depths. Two straight line segments are identified and their slopes used to calculate depths to the corresponding magnetic susceptibility contrasts. For each linear segment, we define three or at least two possible lines, estimate the corresponding depths, and define the

error from these computed depths (h_1 , h_2 , h_r in Fig. 8; see Poudjum Djomani et al., 1995). Mean depths of 0.77 ± 0.15 km and 2.52 ± 0.50 km for the shallow and deep sources, respectively, are determined. The latter predominate at wavenumbers less than 0.2 cycles/km, corresponding to wavelengths longer than 5.0 km. Wavelengths smaller than about 0.6 km represent noise, and possibly some outcropping features. Alternatively, a second straight line segment can be drawn for the shallow sources (h_{s1} and h_{s2} , Fig. 8), with a depth estimate of 0.55 ± 0.10 km. This is larger than the flight height and gives an ensemble depth (from ground surface) of about 0.15 km for these sources, which is $>40\%$ of the grid spacing, and therefore acceptable.

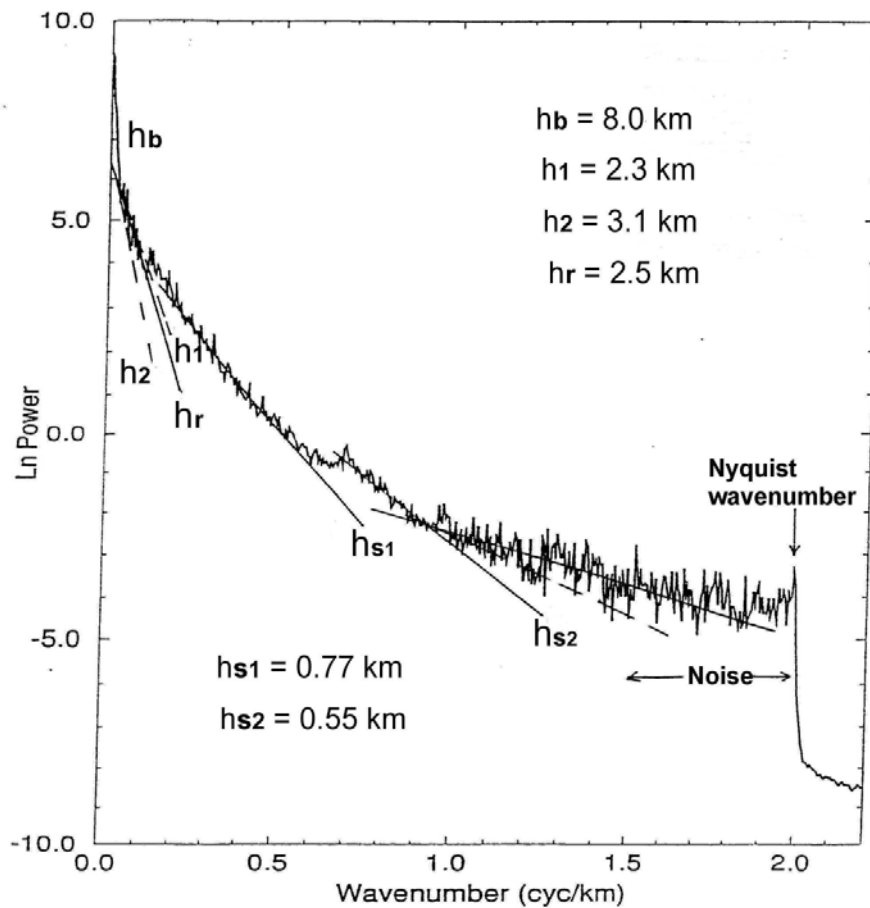


Figure 8. Radially averaged 2D spectra of aeromagnetic data for the study area (h_b = magnetic basement depth; h_r = depth for regional magnetic sources; h_s = depth for shallow sources). Dashed lines show slopes used to estimate error quoted in text following the method of Poudjom-Djomani et al. (1995)

Euler Deconvolution and Spectral Analysis of Regional Aeromagnetic Data from the South-Central Zimbabwe Craton: Tectonic Implications

This shallowest layer may be associated with short wavelength features such as the iron formations, ultramafics and mafic dykes that outcrop in various places within the study area. Comparable results have been obtained in similar granite-greenstone terrains in Australia and Canada (e.g. Hinze, 1985; Cowan and Cowan, 1993). The deepest features (hb, Fig. 8) yield a depth of 8.0 ± 0.5 km below surface, most probably representing the magnetic basement in the area. Significantly, a crustal 'boundary' at a depth of about 7-9 km was estimated from gravity (Ranganai, 1995; Ranganai et al., 2008) and seismic (R. Clark, pers. comm., 1995) data from this area. However, it should be noted that the various techniques 'look' at different parts of the anomaly source and the differences in depths are therefore not unusual. Also, the power spectrum of an area is a statistical estimate such that all spectral estimates are averages. Analysis of spectra covering several magneto-tectonic terrains may produce averages which are not found in either province (Cowan and Cowan, 1993).

For the latter reason, and because the area contains a number of crustal domains where variations in crustal

structure and thickness are expected (Ranganai, 1995; Ranganai et al., 1995), the region has been subdivided into two smaller blocks (north and south of latitude 20.5° S). Figure 9 shows the spectrum for the northern block, corresponding to the northern zone of high magnetic signatures (i.e., the separate terrain discussed earlier). Again, the deep and shallow sources are easily separable but the spectra from the latter show several possible depths. Reliable depths estimates of 4.1 ± 0.50 km are obtained for the deep ensemble (hb) and 0.90 ± 0.20 km for the 'regional' sources (hr). A shallowest layer (hs) at an average depth of 0.4 ± 0.10 km can be determined. Within the defined error limits, this gives depths equal to and greater than the flight height, corresponding to outcropping features in the area. Again, the 4.0 km depth suggests that the basement in the northern area is shallower than in the southern part since the average depth from the overall grid is 8 km. The southern part (south of latitude 20.5° S) could not be evaluated alone due to the interference effects of the NMZ regional anomaly.

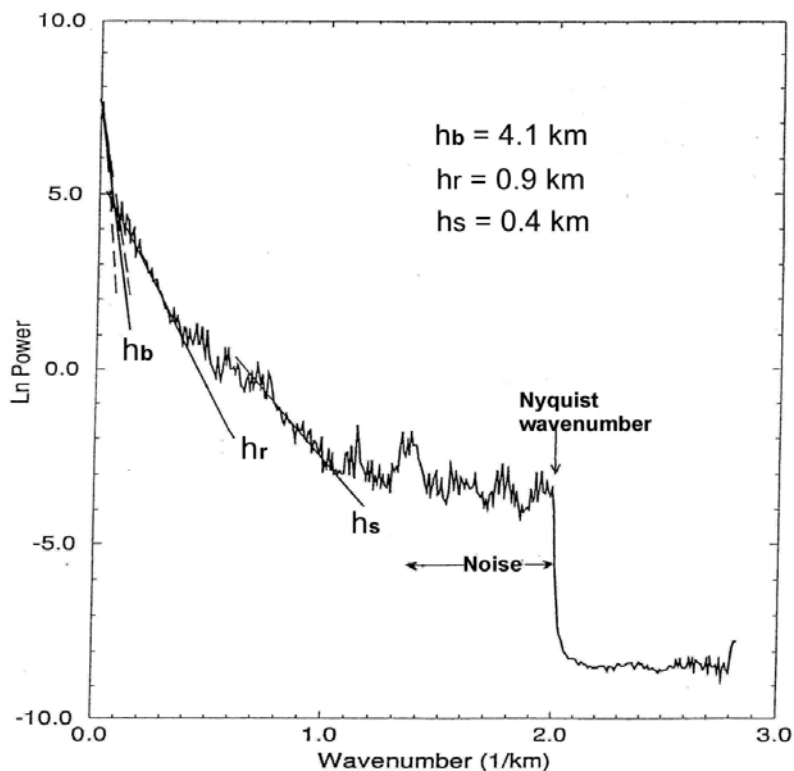


Figure 9. Radially averaged 2D spectra of aeromagnetic data for the northern part of the study area (hb = magnetic basement depth; hr = depth for regional magnetic sources; hs = depth for shallow sources). Dashed lines show slopes used to estimate error quoted in text following the method of Poudjom-Djomani et al. (1995)

SUMMARY AND CONCLUSIONS

Regional aeromagnetic data from the south-central Zimbabwe craton were processed for geological and structural mapping to elucidate the tectonic evolution of the region. Depths to susceptibility contrasts have been determined by spectral analysis and 3D Euler deconvolution, with the latter technique also used for structural interpretation. The well-defined Euler solutions have confirmed the location of both pre-existing and the newly interpreted linear geological features, and gave estimates of their depths, thus confirming the geological significance of the qualitative interpretation. The NNE, NNW, NW, ENE and WNW structures seen on shadow and derivative maps are spatially well-represented by the Euler solutions. The Umvemeela and East dykes appear to extend beyond their mapped exposures into the Limpopo Belt (UD and ED, Figs. 4 and 5). This observation also applies to the Mwenezi fault (Mw) and the interpreted ENE-trending BKD dykes (Figs. 3 to 7). The intersection patterns of all these features provide relative age constraints on the time of crustal extension, dyke intrusion, and the Limpopo orogeny (Table 1). Some new NNE to NE-trending features are defined, particularly in the central-eastern part of the study area. Additional solution patterns suggest the presence of ultramafic sills, which also supports previous qualitative magnetic interpretation and gravity studies (Ranganai, 1995; Ranganai et al., 1995; Ranganai and Ebinger, 2008). Structural and lithologic trends have therefore been established with greater confidence than would be possible by magnetic anomaly-geology correlation alone. For example, a linear cluster of solutions (depth ~2.0 km) mark the ZC-NMZ boundary, confirming geological interpretation of a tectonic contact.

Overall, five major structural trends (regional lineaments) can be identified and associated with the various geological features and craton tectonic events as summarised in Table 1 (cf. Fig. 6), based on previous studies and cross-cutting structures (Ranganai et al., 1995; Ranganai and Ebinger, 2008). The geological-tectonic correlation suggests that the interpreted regional trends are mainly 2.6 Ga and younger, and relate to events including the formation of the Limpopo belt and its subsequent tectonic reactivation

at 2.0 Ga (Kamber et al., 1995; Bumby et al., 2001) and the major regional igneous/ dyking events at 1.8-2.0 Ga (Mashonaland; Wilson et al., 1987; Wilson, 1990), 1.1 Ga (Umkondo; Wilson, 1990; Hanson et al., 1998; Wingate, 2001) and 180 Ma (Karoo; Reeves, 2002; Jones et al., 2001; Le Gall et al., 2002). For example, EW to ESE dykes in the south-western corner form the eastern extension of the >1000 km long Botswana late Karoo Dyke Swarm that has been mapped across northern Botswana (cf. Reeves, 1978, 2000; Wilson et al. 1987; Le Gall et al., 2002). These may constitute a failed third arm of a rift triple junction associated with the break-up of Gondwana, with the Sabi and Lebombo monoclines forming the other two arms (Reeves, 1978, 2000). Ranganai et al. (1995) conclude that the observed structures are due to inter- and intra-cratonic collisions and block movements involving the Zimbabwe and Kaapvaal cratons and the Limpopo Belt, and later crustal extension during the break-up of Gondwana. The movements produced structures, or reactivated older fractures, that were exploited by late Archaean and early Proterozoic mafic intrusions.

Most structures identified are predominantly of shallow origin, with Euler depths solutions of 2.0 km. A number of isolated deep Euler solutions are associated with ultramafic complexes, the Great Dyke and the Umvimeela dyke; and these points could represent the original magma chambers and/or feeder points for these units. There is a general increase in solution depths from north to south which suggests a tilt of the basement in sympathy with the surface terrain (cf. Mushayandebvu, 1995). This probably corresponds to, or reflects, variable uplift and erosion levels between the two halves of the area, separated by the Mchingwe fault. Alternatively, the southern parts could have been affected (tilted?) by loading of the area by Limpopo Belt rocks thrust onto the southern edge of the craton. There are indications of this situation in the spectral analysis results as well, where the northern area yields a shallower depth to magnetic basement than the overall grid. Considering the statistical averaging effect of the technique, the results mean that the magnetic basement in the southern parts should be much deeper than the overall grid result suggests.

**Euler Deconvolution and Spectral Analysis of Regional Aeromagnetic Data from
the South-Central Zimbabwe Craton: Tectonic Implications**

Table 1. Major Aeromagnetic Structural Trends and their Geological Association.

(After Ranganai et al., 1995; Ranganai and Ebinger, 2008) (See Figs. 2 to 6 for comparison)

Trend/Direction	Geological Features/Craton Tectonic Events and Timing
E-W to ESE/WNW	Botswana Karoo Dyke swarm, BKD; Plumtree dyke swarm (Gondwana break-up: Reeves, 1978, 2000; Wilson et al, 1987; Le Gall et al., 2002) 170-200 Ma
ENE/WSW	Sabi-Limpopo dyke swarm (Karoo Igneous event; Wilson et al. 1987; Reeves, 2000; Le Gall et al., 2002) 170-200 Ma
Dolerite sills (Not in study area)	Umkondo Igneous event (Wilson, 1979, 1990; Wilson et al., 1987; Hanson et al., 1998). 1100 Ma
NNW/SSE	Sebanga Poort Dyke set, including Filabusi and Fort Rixon dykes, FRD. (Mashona land Igneous Event: Wilson, 1979, 1981; Wilson et al. 1987). 1800-2000 Ma
NW/SE	Mchingwe/Jenya/Mwenezi faults plus others (Dextral shear couple acting on craton- Wilson, 1990; Campbell et al., 1992). ~2000 Ma
NNE/SSW	Great Dyke, East and Umvimeela dyke, plus Popoteke fault set (Great Dyke Fracture System: Wilson, 1979, 1990). 2500 Ma
ENE/WSW	NMZ, Chivi/Razi granites, (LB overthrust onto ZC: Van Reenen et al. 1992; Mkweli et al., 1995; Frei et al., 1999) ~2600 Ma

Spectral analysis of the magnetic data shows that there are generally three statistical populations of magnetic sources: features at average depths of 0.5 to 1.0 km, 'deep' sources between 2.0 and 4.0 km, and regional features at 8.0 km. Except for the last depth which most probably maps the magnetic basement in the area, these results are comparable to estimates from Euler deconvolution, where average depths of 0.5, 1.0 and 2.5 km are obtained. The shallowest depths can be easily associated with the known geological units: the out-cropping and near surface (i.e. sub-cropping) features such as mafic dykes, iron formation horizons in greenstone belts, and ultramafic intrusions. Significantly, magnetic modelling of several profiles across the Umvimeela and East dykes have yielded depths generally ranging from 100 m to 300 m (Mushayandebvu, 1995). This lends support to our results for the shallowest features, particularly the magnetic dykes as well as the BIF and ultramafic horizons within the greenstone belts. The magnetic basement depth of 8 km corresponds to the crustal boundary estimated at about 7-9 km from gravity and seismic data. An important implication is that the

greenstone belts were an integral part of the lithosphere before much of the upper crustal (brittle) deformation occurred. The geostructural framework of the area is compatible with the postulated late Archaean collision involving the Zimbabwe and Kaapvaal cratons and the Limpopo Belt, and later crustal extension during the break-up of Gondwana.

ACKNOWLEDGEMENTS

Edgar Stettler, Oswald Gwavava and Sue Webb are thanked for their constructive comments on an earlier version of the paper. Advice and encouragement given by Dai Jones and Alan Reid at various stages of the study is greatly appreciated. The Zimbabwe Geological Survey provided the aeromagnetic data and gave permission for the data to be published. The study benefited from the British Council Link Scheme between the Departments of Earth Sciences (University of Leeds) and Physics (University of Zimbabwe).

REFERENCES

- Allek, K., Mohamed Hamoudi, M., 2008. Regional-scale aeromagnetic survey of the south-west of Algeria: A tool for area selection for diamond exploration. *Journal of African Earth Sciences* **50**, 67–78
- Barbosa, V. C. F., Silva, J. B. C., and Medeiros, W. E., 1999. Stability analysis and improvement of structural index estimation in Euler deconvolution: *Geophysics* **64**, 48–60.
- Barritt, S.D., 1993. The African Magnetic Mapping Project, *ITC Journal* 1993-2, 122-131.
- Bates, M. P. and Mushayandebvu, M. F., 1995. Magnetic fabric in the Umvimeela Dyke, satellite of the Great Dyke, Zimbabwe. *Tectonophysics* **242**, 241-254.
- Bickle, M. J. and Nisbet, E. G. (Eds.), 1993. The geology of the Belingwe greenstone belt, Zimbabwe: A study of the evolution of Archaean continental crust. Geological Society Zimbabwe Special Publication **2**, 239p. A. A. Balkema, Rotterdam.
- Blakely, R. J., 1995. *Potential Theory in Gravity and Magnetic Applications*. 441p. Cambridge.
- Blenkinsop, T.G., Martin, A., Jelsma, H.A., Vinyu, M.L., 1997. The Zimbabwe Craton. In: de Wit, M.J., Ashwal, L.D. (Eds.), *Greenstone Belts*. Oxford monograph on geology and geophysics, Oxford University Press, Oxford, p. 567-580.
- Bournas, N., Galdeano, A., Hamoudi, M., Baker, H., 2003. Interpretation of the aeromagnetic map of Eastern Hoggar (Algeria) using the Euler deconvolution, analytic signal and local wavenumber methods. *Journal of African Earth Sciences* **37**, 191–205
- Bumby, A.J., Eriksson, P.G., Van Der Merwe, R., Brümmer, J.J., 2001. Shear-zone controlled basins in the Blouberg area, Northern Province, South Africa: syn- and post-tectonic sedimentation relating to ca. 2.0 Ga reactivation of the Limpopo Belt. *Journal of African Earth Sciences* **33**, 445-461
- Campbell, S.D.G., Oesterlen, P.M., Blenkinsop, T.G., Pitfield, P.E.J. and Munyanyiwa, H. 1992. A Provisional 1:2 500 000 scale Tectonic map and the tectonic evolution of Zimbabwe. *Annals of the Zimbabwe Geological Survey*, **XVI** (1991), 31-50.
- Cowan, D. R. and Cowan, S., 1993. Separation filtering applied to aeromagnetic data. *Exploration Geophysics* **24**, 429-436.
- Fairhead, D.J., Bennett, K., Gordon, D.H. and Huang, D., 1994. EULER: beyond the black-box. 64th Annual International Meeting, Society of Exploration Geophysicists, Expanded Abstracts, 422-424.
- Fedo, C.M., Eriksson, K. and Blenkinsop, T.G. 1995. Geologic history of the Archean Buhwa Greenstone Belt and surrounding granite-gneiss terrane, Zimbabwe, with implications for the evolution of the Limpopo Belt. *Canadian Journal of Earth Sciences*, **32**, 1977-1990.
- Frei, R., Blenkinsop, T.G., and Schönberg, R., 1999, Geochronology of the late Archaean Razi and Chilimanzi suites of granites in Zimbabwe: implications for the late Archaean tectonics of the Limpopo belt and Zimbabwe craton: *South African Journal of Geology* **102**, 55-63.
- Geosoft, 2004. Oasis Montaj (V5.1.8) and Euler 3D Deconvolution System (V5.1.5) manuals. Geosoft Inc., Toronto. Canada.
- Grant, F. S., 1985. Aeromagnetics, geology and ore environments, I. Magnetite in igneous, sedimentary and metamorphic rocks: an overview. *Geoexploration* **23**, 303-333.
- Gwavava, O., Swain, C.J., Podmore, F. and Fairhead, I.D., 1992. Evidence of crustal thinning beneath the Limpopo Belt and Lebombo monocline of southern Africa based on regional gravity studies and implications for the reconstruction of Gondwana. *Tectonophysics* **212**, 1-20.
- Hahn, A., Kind, E.G., and Mishra, D.C., 1976. Depth estimation of magnetic sources by means of Fourier amplitude spectra. *Geophysical Prospecting* **24**, 287-308.
- Hanson, R.E., Martin, M.W., Bowring, S.A., Munyanyiwa, H., 1998. U–Pb zircon age for the Umkondo dolerites, eastern Zimbabwe: 1.1 Ga large igneous province in southern Africa–east Antarctica and possible Rodinia correlations. *Geology* **12**, 1143–1146.
- Hickman, M. H., 1978. Isotopic evidence for crustal reworking in the Rhodesian Archaean craton, southern Africa. *Geology* **6**, 214-216.
- Hinze, W. J. (Ed.), 1985. *The utility of regional gravity and magnetic anomaly maps*. Society Exploratin Geophysicists. Tulsa. 454p.
- Horstwood, M.S.A., Nesbitt, R.W., Noble, S.R. and Wilson, J.F., 1999. U-Pb zircon evidence for an extensive early Archean craton in Zimbabwe: a reassessment of the timing of craton formation, stabilization and growth. *Geology* **27**, 707-710.
- Jelsma, H.A., Dirks, P.H.G.M., 2002. Neoproterozoic tectonic evolution of the Zimbabwe Craton. In Fowler, C.M.R., Ebinger, C., Hawkesworth, C.J. (Editors), *The Early Earth: Physical, Chemical and Biological Development*. Geological Society of London, *Special Publications*, **199**, 183-211.

**Euler Deconvolution and Spectral Analysis of Regional Aeromagnetic Data from
the South-Central Zimbabwe Craton: Tectonic Implications**

- Jelsma, H.A., Vinyu, M.L., Valbracht, P.J., Davies, G.R., Wijbrans, J.R., Verdurmen, E.A.T., 1996. Constraints on Archaean crustal evolution of the Zimbabwe craton: U-Pb zircon, Sm-Nd and Pb-Pb whole-rock isotope study. *Contribution Mineralogy and Petrology* **124**, 55-70.
- Jones, D.L., Bates, M.P., Podmore, F. and Mushayandebvu, M.F., 1995. The Great Dyke of Zimbabwe and Its Satellites: Recent Geophysical Results and Their Implications. In: Srivastava, R.K. and Chandra, R. (Eds), *Magmatism in Relation to Diverse Tectonic Settings*, Oxford and IBH Publishing Co. Pvt. Ltd, p209-222.
- Jones, D.L., Duncan, R.A., Briden, J.C., Randall, D.E., MacNiocail, C., 2001. Age of the Batoka basalts, northern Zimbabwe, and the duration of Karoo large igneous province magmatism, *G3 Geochemistry, Geophysics, Geosystems* **2**, 1–15.
- Kamber, B.S., Kramers, J.D., Napier, R., Cliff, R.A. and Rollinson, H.R. 1995. The Triangle Shearzone, Zimbabwe, revisited: new data document an important event at 2.0 Ga. in the Limpopo Belt. *Precambrian Research* **70**, 191-213.
- Kusky, T.M., 1998. Tectonic setting and terrane accretion of the Archaean Zimbabwe craton. *Geology* **26**, 163-166.
- Le Gall, B., Tshoso, G., Jourdan, F., Fe'raud, G., Bertrand, H., Tiercelin, J.J., Kampunzu, A.B., Modisi, M.P., Dymant, J., Maia, M., 2002. $^{40}\text{Ar}/^{39}\text{Ar}$ geochronology and structural data from the giant Okavango and related mafic dyke swarms, Karoo igneous province, Botswana. *Earth and Planetary Science Letters* **202**, 595–606.
- McDonald, A. J. W., Fletcher, C. J. N., Carruthers, R. M., Wilson, D. and Evans, R. B., 1992. Interpretation of the regional gravity and magnetic surveys of Wales, using shaded relief and Euler deconvolution techniques. *Geological Magazine* **129**, 523-531.
- Mkweli, S., Kamber, B. and Berger, M. 1995. Westward continuation of the craton-Limpopo Belt tectonic break in Zimbabwe and new age constraints on the timing of the thrusting. *Journal of the Geological Society, London* **152**, 77-83.
- Mukasa, S.B., Wilson, A.H. and Carlson, R.W. 1998. A multielement geochronologic study of the Great Dyke, Zimbabwe: significance of the robust and reset ages. *Earth and Planetary Science Letters* **164** (1/2), 353-369.
- Mushayandebvu, M. F., 1995. Magnetic modelling of the Umvimeela and East dykes: Evidence for regional tilting of the Zimbabwe craton adjacent to the Limpopo Belt. *Journal of Applied Science in Southern Africa* **1**, 47-58.
- Mushayandebvu, M. F., van Driel, P., Reid, A.B., and Fairhead, J.D., 2001. Magnetic source parameters of two dimensional structures using extended Euler deconvolution: *Geophysics* **66**, 814-823.
- Mushayandebvu, M.F., Lesurz, V., Reid, A.B., Fairhead, D.J., 2004. Grid Euler deconvolution with constraints for 2D structures. *Geophysics* **69**(2), 489–496
- Nisbet, E.G. 1987. *The Young Earth: an introduction to Archaean geology*. Boston, Allen and Unwin, 402p.
- Oberthür, T.; Davis, D. W.; Blenkinsop, T. G; and Höhndorf, A. 2002. Precise U-Pb mineral ages, Rb-Sr and Sm-Nd systematics of the Great Dyke, Zimbabwe: constraints on late Archean events in the Zimbabwe Craton and Limpopo Belt. *Precambrian Research* **113**: 293–305.
- Paterson, N. R., Kwan, K. C. H. and Reford, S. W., 1992. Use of Euler deconvolution in recognizing magnetic anomalies of pipelike bodies. 62nd Annual International Meeting, Society of Exploration Geophysicists, SEG Expanded Abstracts, Volume 1, 642-645.
- Podmore, F. and Wilson, A. H., 1987. A reappraisal of the structure and geology of the Great Dyke, Zimbabwe. In: Halls, H. C. and Fahrig, W. F. (Eds.), *Mafic Dyke Swarms*. Geological Association Canada, Special Paper 33, 317-330.
- Poudjom-Djomani, Y. H., Ebinger, C. E. Diament, M., Fairhead, J. D., 1995. Effective elastic thickness variations in West-Central Africa inferred from gravity data. *Journal of Geophysical Research* **100**(B11), 22047-22070.
- Prendergast, M.D., 2004. The Bulawayan Supergroup: a late Archaean passive margin-related large igneous province in the Zimbabwe craton. *Journal of the Geological Society* **161**(3): 431 - 445.
- Prendergast, M.D., Wingate, M.T.D., 2007. Zircon geochronology and partial structural re-interpretation of the late Archaean Mashaba Igneous Complex, south-central Zimbabwe. *South African Journal of Geology* **110**(4), 585-596.
- Ranganai, R.T., 1995. Geophysical Investigations of the Granite-Greenstone Terrain in the South-Central Zimbabwe Archaean Craton. Ph D Thesis 288p, University of Leeds, Leeds, UK.
- Ranganai, R.T. 1999. Structure and Depth Mapping in the south-central Zimbabwe Craton using 3D Euler Deconvolution and Spectral Analysis of Regional Aeromagnetic Data. *Journal of African Earth Sciences* **28**(4A), 67-68.
- Ranganai, R.T. and Ebinger, C.J., 2008. Aeromagnetic and LANDSAT TM Structural Interpretation for Identifying Regional Groundwater Exploration Targets, South-Central Zimbabwe Craton. *Journal of Applied Geophysics* (in press).

- Ranganai, R.T., Whaler, K.A. and Ebinger, C.E. 2008. Gravity anomaly patterns in the south-central Zimbabwe (Archaean) craton and their geological interpretation. *Journal of African Earth Sciences* **51** (In press). <http://dx.doi.org/10.1016/j.jafrearsci.2008.01.011>
- Ranganai, R. T., Whaler, K. A., Ebinger, C. E., Stuart, G. W., 1995. Crustal structure of the south-central Zimbabwe Archaean craton from Gravity and Aeromagnetic data: Implications for tectonic evolution. *EAGE Extended Abstracts*, Paper D28, Glasgow.
- Reeves, C. V., 1978. A failed Gondwana spreading axis in southern Africa. *Nature* **273**, 222-223.
- Reeves, C. V. 2000. The geophysical mapping of Mesozoic dyke swarms in southern Africa and their origin in the disruption of Gondwana. *Journal of African Earth Sciences* **30**, 499-513.
- Reid, A. B., Allsop, J. M., Granser, H., Millet, A. J. and Somerton, I. W., 1990. Magnetic interpretation in three dimensions using Euler deconvolution. *Geophysics* **55**, 80-91.
- Rollinson, H.R. and Blenkinsop, T.G. 1995. The magmatic, metamorphic and tectonic evolution of the Northern Marginal Zone of the Limpopo Belt in Zimbabwe. *Journal of the Geological Society of London* **152**, 65-75.
- Ruotoistenmaki, T., 1983. Depth estimation from potential field data using the Fourier amplitude spectra. *Geoexploration* **21**, 191-201.
- Ruotoistenmaki, T., 1987. Estimation of depth to potential field sources using the Fourier amplitude spectrum. *Geological Survey Finland, Bulletin* **340**, 84p.
- Schoenberg, R., Nägler, T.F., Gnos, E., Kramers, J.D., Kamber, B.S., 2003. The source of the Great Dyke, Zimbabwe, and its tectonic significance: evidence from Re-Os isotopes. *Journal of Geology* **111**, 565-578.
- Spector, A. and Grant, F. S., 1970. Statistical models for interpreting aeromagnetic data. *Geophysics* **35**, 293-302.
- Spector, A. and Grant, F. S., 1975. Comments on 'Two-dimensional Power Spectral Analysis of Aeromagnetic Fields'. *Geophysical Prospecting* **23**, 391.
- Spector, A. and Parker, W., 1979. Computer compilation and interpretation of geophysical data. *Geological Survey Canada*, Economic Geology Report 31, 527-544.
- Smith, W.H.F., Wessel, P., 1990. Gridding with continuous curvature splines in tension. *Geophysics* **55**, 293-305.
- Taylor, P.N., Kramers, D.J., Moorbath, S., Wilson, J.F., Orpen, J.L. and Martin, A. 1991. Pb/Pb, Sm-Nd and Rb-Sr geochronology in the Archaean craton of Zimbabwe. *Chemical Geology (Isotope Geosciences)* **87**, 175-196.
- Thompson, D. T., 1982. EULDPH: a new technique for computer-assisted depth estimates from magnetic data. *Geophysics* **47**, 31-37.
- Van Reenen, D. D., Roering, C., Ashwal, L. D. and de Wit, M. J. (Eds.), 1992. The Archaean Limpopo granulite belt: Tectonics and deep crustal processes. *Precambrian Research* **55**, 1-587.
- Wilson, A. H. and Prendergast, M. D., 1988. The Great Dyke of Zimbabwe-I: tectonic setting, stratigraphy, petrology, structure, emplacement and crystallization. In: Prendergast, M. D. and Jones, M. J. (Eds.), *Magmatic Sulphides- the Zimbabwe Volume*, pp1-20. Institute of Mining and Metallurgy.
- Wilson, J. F. 1979. A preliminary reappraisal of the Rhodesian Basement Complex. Geological Society of South Africa Special Publication 5, 1-23.
- Wilson, J. F., 1981. The granite-gneiss greenstone shield, Zimbabwe. In: Hunter, D. R. (Ed.), *Precambrian of the southern hemisphere*, Elsevier, 454-488.
- Wilson, J. F., 1990. A craton and its cracks: some of the behaviour of the Zimbabwe block from the Late Archaean to the Mesozoic in response to horizontal movements, and the significance of some of its mafic dyke fracture patterns. *Journal African Earth Sciences* **10**, 483-501.
- Wilson, J. F., Jones, D. L. and Kramers, J. D., 1987. Mafic dyke swarms in Zimbabwe. In: Halls, H.C. and Fahrig, W.F. (Eds.), *Mafic Dyke Swarms*. Geological Association Canada, Special Paper **33**, 433-444.
- Wilson, J.F., Nesbitt, R.W. and Fanning, C.M. 1995. Zircon geochronology of Archaean felsic sequences in the Zimbabwe craton: a revision of greenstone stratigraphy and a model for crustal growth. In: Coward, M.P. & Ries, A.C. (Eds.), *Early Precambrian Processes*, Geological Society Special Publication **95**, 109-126.
- Wingate, M.T.D., 2001. SHRIMP baddeleyite and zircon ages for an Umkondo dolerite sill, Nyanga Mountains, Eastern Zimbabwe. *South African Journal of Geology* **104**, 13-22.